

Third-order nonlinearity by the inverse Faraday effect in planar magnetoplasmonic structures

Song-Jin Im,^{1,*} Chol-Song Ri,¹ Kum-Song Ho,¹ and Joachim Herrmann^{2,†}

¹*Department of Physics, Kim Il Sung University, Taesong District,
Pyongyang, Democratic People's Republic of Korea*

²*Max-Born-Institute for Nonlinear Optics and Short Pulse Spectroscopy, Max-Born-Str. 2a, D-12489 Berlin, Germany*
(Dated: February 21, 2022)

We predict a new type of ultrafast third-order nonlinearity of surface plasmon polaritons (SPP) in planar magneto-plasmonic structures caused by the inverse Faraday effect (IFE). Planar SPPs with a significant longitudinal component of the electric field act via the IFE as an effective transverse magnetic field. Its response to the plasmon propagation leads to strong ultrafast self-action which manifests itself through a third-order nonlinearity. We derive a general formula and analytical expressions for the IFE-related nonlinear susceptibility for two specific planar magneto-plasmonic structures from the Lorentz reciprocity theorem. Our estimations predict a very large nonlinear third-order nonlinear susceptibility exceeding those of typical metals such as gold.

PACS numbers: 42.65.-k, 73.20.Mf, 75.78.jp, 78.20.Ls

I. INTRODUCTION

Nonlinear optical effects can be enhanced by plasmonic structures supporting local field enhancement and inhomogeneity on the nanoscale¹. In particular, nonlinear propagation of surface plasmon polaritons (SPPs) in plasmonic waveguides has attracted attention to achieve ultrafast phase modulation and due to its implication for plasmonic systems^{2,3}. Different types of nonlinear plasmonic waveguides has been theoretically investigated, such as nonlinear plasmonic planar waveguides⁴⁻⁷, metal nanowires^{8,9}, slot waveguides¹⁰ and periodic waveguides^{11,12}. In such plasmonic waveguides, the effective nonlinearity originates from the third-order optical Kerr effect describing a refractive index change proportional to the square of the absolute value of the electric field strength.

Recently, manipulation of the magnetic order of thin magnetic films by ultrashort pulses based on the inverse Faraday effect (IFE) has attracted much attention because of its potential impact for future data storage, spintronics¹³⁻¹⁵ and improved imaging¹⁶⁻¹⁹. Using field enhancement plasmonic structures has also been studied for the enhancement of the IFE²⁰⁻²² and to achieve control of the magnetization of ferromagnetic material on the nanoscale¹⁹. On the other hand, in the last years much effort has been devoted to study new ways to control the properties of surface plasmons using external magnetic fields in ferromagnetic dielectric²³ or metal²⁴ layers. In these experiments the magnetization induced by the external magnetic field leads to a change of the plasmon wavenumber which can be measured by a plasmonic double-slit interferometer.

In this paper we theoretically predict a new type of ultrafast third-order nonlinearity of surface plasmon polaritons in planar ferromagnetic plasmonic structures related with the inverse Faraday effect. In a plasmonic layer, planar SPP with a longitudinal component of the electric

field induce a magnetization which leads to a third-order nonlinear polarization. This kind of nonlinearity plays in the plasmon propagation analog effects as the optical Kerr effect but it originates from a different physical mechanism. We derive a formula for the IFE-related nonlinear susceptibility and explicit analytical expressions for two kinds of planar magneto-plasmonic structures. The IFE-related nonlinear susceptibility differs from the traditional Kerr-related nonlinear susceptibility by its magnitude, frequency dependence and its inherent dependence on the material parameters.

II. IFE-RELATED THIRD-ORDER NONLINEAR SUSCEPTIBILITY FOR PLANAR MAGNETO-PLASMONIC STRUCTURES

In a bulk ferromagnetic material, a static external magnetic field leads to a magnetization $\vec{M} = \vec{M}(\vec{H})$ ²⁵. In such material the vector of the electric displacement depends on the external magnetic field and is described by

$$\vec{D} = \epsilon_0 \hat{\epsilon} \vec{E} = \epsilon_0 \left(\epsilon \vec{E} + i\beta \vec{E} \times \vec{M} \right), \quad (1)$$

where the relative permittivity tensor $\hat{\epsilon}$ is expressed as

$$\hat{\epsilon} = \begin{pmatrix} \epsilon & i\beta M_z & -i\beta M_y \\ -i\beta M_z & \epsilon & i\beta M_x \\ i\beta M_y & -i\beta M_x & \epsilon \end{pmatrix}$$

and β describes the magneto-optical susceptibility. From this relation one can see that the optical polarization has a contribution proportional to the magnetization \vec{M} . The consequence of this relationship is the magneto-optical Faraday effect leading to a polarization rotation when a linearly polarized light beam is transmitted through a magneto-optical medium under an external magnetic field. The non-diagonal terms in the permittivity tensor

describes also the changes to light reflected from a magnetized surface (magneto-optical Kerr effect, MOKE). Pump-probe measurement in nickel films has shown that fast subpicosecond demagnetization can be induced by femtosecond optical pulses²⁶.

A magnetic material irradiated by circularly polarized light induces a magnetization along the wave vector \vec{k} ^{27,28} which is called the inverse Faraday effect (IFE). The light-induced magnetization can be expressed as

$$\vec{M} = -i\chi(\vec{E} \times \vec{E}^*) \quad (2)$$

where $\chi = \chi_g^{(3)}/\beta$ is a material dependent constant related with the Verdet constant and $\chi_g^{(3)}$ can be understood as the IFE-related third-order nonlinear susceptibility of the bulk ferromagnetic material. Left- and right-handed polarization waves induce magnetization of opposite signs.

Light cannot penetrate into a thin metallic layer, but under appropriate conditions (as e.g. by using the Kretschman configuration for p-polarized light) surface plasmon-polaritons (SPP) can be excited moving along the surface. Plasmons exhibit a longitudinal component of the electric field, therefore the chirality $\vec{E} \times \vec{E}^*$ of plasmons do not vanishes. This means that even for a linearly polarized input beam a magnetization can be induced by plasmons, but the polarization of the plasmon is not circularly polarized.

Substituting the expression (2) for the magnetization into relation (1) we can see that the IFE leads to a third-order nonlinear polarization caused by a different physical mechanism than the optical Kerr effect. For the derivation of the IFE-related nonlinear susceptibility of a planar plasmonic structures including a ferromagnetic layer, we use a formalism similar as in Ref.⁹. In a planar waveguides the electromagnetic field is confined in different spatial modes²⁹, but only the fundamental mode plays here a role. The mode expansion for the electric and the magnetic fields $\vec{F} = (\vec{E}; \vec{H})$ in the plasmonic waveguide can be expressed as $\vec{F}(\vec{r}, t) = (1/2) \cdot [\vec{F}(\vec{r}) \exp(-i\omega t) + \text{c.c.}]$, where c.c. signifies the complex conjugate. Below, we restrict ourselves to the time-independent amplitude for the fundamental mode, $\vec{F}(\vec{r})$, which can be expressed as

$$\vec{E}(\vec{r}) = \sqrt{1/s_0} \Psi(x) \exp(i\kappa x) \vec{e}_0(\vec{r}_\perp), \quad (3)$$

$$\begin{aligned} \vec{H}(\vec{r}) &= (i\omega\mu_0)^{-1} \nabla \times \vec{E} \\ &= \sqrt{1/s_0} \Psi(x) \exp(i\kappa x) \vec{h}_0(\vec{r}_\perp). \end{aligned} \quad (4)$$

Here x and \hat{x} are the coordinate and the unit vector in the direction of propagation, \vec{r}_\perp is the position vector in the transverse plane, s_0 is defined as $s_0 = (1/2) \int \text{Re}(\vec{e}_0 \times \vec{h}_0^*) \cdot \hat{x} d\sigma$, where the integral is performed over the transverse plane, $k = \kappa + i\alpha/2$ is the SPP propagation constant, Ψ is normalized so that the

$|\Psi|^2$ is equal to the power flow along the x direction $P(x) = (1/2) \int \text{Re}(\vec{E} \times \vec{H}^*) \cdot \hat{x} d\sigma = |\Psi|^2$, and $\vec{e}_0(\vec{r}_\perp)$ and $\vec{h}_0(\vec{r}_\perp)$ describe the spatial transverse distribution of the mode. We start from the Lorentz reciprocity theorem³⁰

$$\begin{aligned} &\frac{\partial}{\partial x} \int [\vec{E}_1(\vec{r}) \times \vec{H}_2(\vec{r}) - \vec{E}_2(\vec{r}) \times \vec{H}_1(\vec{r})] \cdot \hat{x} d\sigma \\ &= i\omega \int (\vec{E}_1(\vec{r}) \cdot \vec{D}_2(\vec{r}) - \vec{E}_2(\vec{r}) \cdot \vec{D}_1(\vec{r})) d\sigma, \end{aligned} \quad (5)$$

where (\vec{E}_1, \vec{H}_1) and (\vec{E}_2, \vec{H}_2) are two arbitrary guided modes. Now we substitute for (\vec{E}_1, \vec{H}_1) and (\vec{E}_2, \vec{H}_2) the unperturbed backward propagating field $(\vec{E}_0^-, \vec{H}_0^-)$ and the perturbed forward propagating field (\vec{E}, \vec{H}) depending on an external quasi-static transverse magnetic field H_{ex} , correspondingly. The external magnetic field induces a magnetization $\vec{M} = (0, M, 0)$, $M = M(H_{ex})$ in the transverse y-direction and leads to a perturbation for the mode distribution. In the first order of perturbation Eq. (5) leads to the following equation describing the amplitude $\Psi(x)$ of the plasmonic field:

$$\frac{d\Psi}{dx} = -\frac{\alpha}{2} \Psi + i\Delta k \cdot \Psi, \quad (6)$$

where α is the linear loss coefficient and

$$\Delta k = \frac{ik_0\beta \int M \cdot e_{0x} e_{0z} d\sigma}{Z_0 \int (\vec{e}_0 \times \vec{h}_0) \cdot \hat{x} d\sigma} \quad (7)$$

is the shift of the plasmon wavenumber induced by the external magnetic field. $Z_0 = \sqrt{\mu_0/\epsilon_0}$ and $k_0 = 2\pi/\lambda$ are the wave impedance and the light wavenumber in vacuum, respectively.

Now we consider an alternative arrangement without external static magnetic field but with a laser pulse directed to the planar magneto-optical structure and acting as an effective magnetic field via the IFE. The SPP mode of the planar plasmonic waveguide induces a magnetization into the transverse y-direction. From Eq. (2) the nonlinear magnetization $\vec{M} = (0, M, 0)$ is expressed as

$$M = -i\chi(E_x^* E_z - E_x E_z^*) \quad (8)$$

with $\chi = \chi_g^{(3)}/\beta$. If we substitute Eq. (8) into Eq. (6) and (7), we find

$$\frac{d\Psi}{dx} = -\frac{\alpha}{2} \Psi + i\gamma |\Psi|^2 \Psi, \quad (9)$$

where

$$\gamma = k_0 \frac{2 \int \chi_g^{(3)} e_{0x} e_{0z} (e_{0x}^* e_{0z} - e_{0x} e_{0z}^*) d\sigma}{Z_0 \int (\vec{e}_0 \times \vec{h}_0) \cdot \hat{x} d\sigma \cdot \int \text{Re}(\vec{e}_0 \times \vec{h}_0^*) \cdot \hat{x} d\sigma}, \quad (10)$$

is the effective nonlinear propagation coefficient.

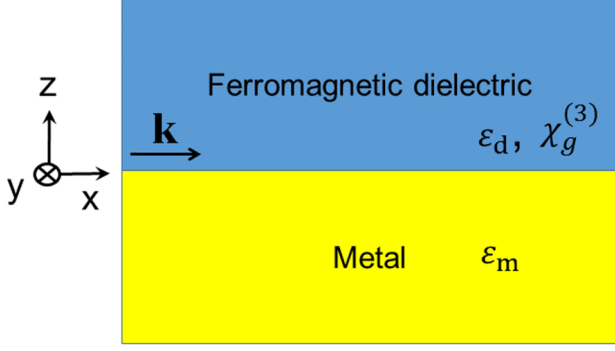


FIG. 1. The ferromagnetic dielectric/metal interface.

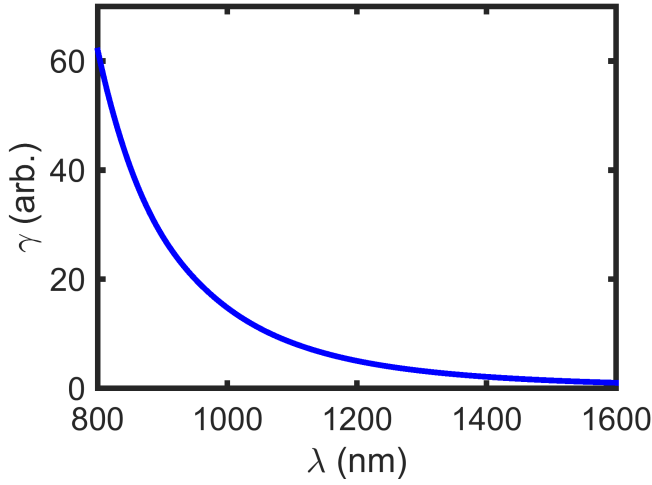


FIG. 2. Wavelength-dependence of the IFE-related nonlinear susceptibility for the interface between gold and a ferromagnetic dielectric. The nonlinear susceptibility of the bulk ferromagnetic dielectric $\chi_g^{(3)}$ is assumed to be independent on the wavelength.

III. FERROMAGNETIC DIELECTRIC/METAL INTERFACE

Let us derive more explicit analytical formulas for two typical types of planar magneto-plasmonic interfaces. First, we consider a ferromagnetic dielectric/metallic interface as shown in the Fig. 1.

In the case that an external magnetic field H_{ex} is present leading to a magnetization $M = M(H_{ex})$, by substituting the analytical expression of the fundamental TM mode distribution of a single interface Eq. (2.10)-(2.14) of Ref.²⁹ into Eq. (7) we can derive a plasmon wavenumber shift given by

$$\Delta k = k_0 \frac{\beta M}{\sqrt{-(\epsilon_m + \epsilon_d)(1 - \epsilon_d^2/\epsilon_m^2)}}. \quad (11)$$

Eq. (11) is in agreement with Eq. (4) of Ref.²³ used for

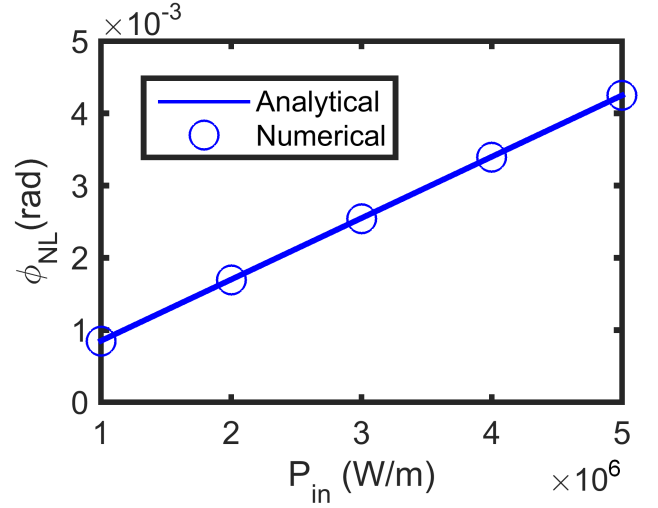


FIG. 3. Power-dependence of the nonlinear phase shift for a wavelength of 1550 nm and a propagation distance of $L=1000$ nm for the interface between gold and a ferromagnetic dielectric with $\epsilon_d = 4$. The blue line represents $\phi_{NL} = \gamma PL$ using the analytical formula of γ by Eq. (12). The blue circles represent $\phi_{NL}(P) = \phi(P_{in} = P) - \phi(P_{in} \rightarrow 0)$ calculated by the numerical solutions of Maxwell equations in the frequency domain. Here we assumed $\chi_g^{(3)} = 10^{-17} \text{m}^2 \text{V}^{-2}$.

the description of the control of the optical phase of a plasmon in a magneto-optical interferometer.

For the case without external magnetic field but with an incident laser pulse the substitution of the analytical mode distribution for the fundamental mode of the planar plasmonic waveguide²⁹ into Eq. (10) yields the following expression:

$$\gamma \approx \frac{-4\chi_g^{(3)}}{c\epsilon_0} \frac{\epsilon_m^4 \epsilon_d}{(\epsilon_m^2 - \epsilon_d^2)^2 (\epsilon_m + \epsilon_d)} \sqrt{\frac{-1}{\epsilon_m + \epsilon_d}} k_0^2. \quad (12)$$

Here, high quality of the plasmonic metal was assumed so that $\text{Im}\epsilon_m \ll |\text{Re}\epsilon_m|$.

Fig. 2 shows the wavelength-dependence of the nonlinear coefficient γ . Here, we used the frequency-depending experimental data for the permittivity of gold³¹ as $\epsilon_m(\lambda)$. The wavelength-dependence of the nonlinear susceptibility of the bulk ferromagnetic dielectric $\chi_g^{(3)}$ is disregarded.

Fig. 3 shows the power-dependence of the nonlinear phase shift ϕ_{NL} for a wavelength of 1550 nm and a propagation distance of $L = 1000$ nm for an interface between gold and a ferromagnetic dielectric. For the calculation of the absolute values of the nonlinear phase shift, we assumed $\chi_g^{(3)} = 10^{-17} \text{m}^2 \text{V}^{-2}$ and $\epsilon_d = 4$. The blue line represents $\phi_{NL} = \gamma PL$ with the analytical prediction of γ by Eq. (12). The analytical prediction is in good agreement with the numerically determined phase shift $\phi_{NL}(P) = \phi(P_{in} = P) - \phi(P_{in} \rightarrow 0)$ (the blue circles in Fig. 4), obtained by numerical solutions of the Maxwell equations in the frequency domain (analogous

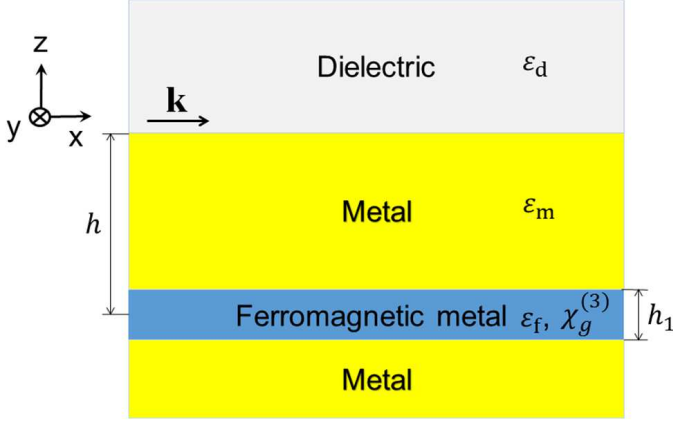


FIG. 4. The dielectric/hybrid metal-ferromagnet interface.

as in Ref. ⁹).

If we consider $\varepsilon_d \ll |\varepsilon_m|$ in the infrared region, Eq. (12) is simplified to

$$\gamma \approx \frac{4\chi_g^{(3)}k_0^2}{c\varepsilon_0} \frac{\varepsilon_d}{(-\varepsilon_m)^{3/2}}. \quad (13)$$

The IFE-related nonlinear susceptibility is predicted to be linearly dependent on the permittivity of the dielectric material as can be seen in Eq. (13). Note that for the same material besides the IFE-related third-order nonlinearity a different type of third-order nonlinearity exist caused by the optical Kerr effect. Substituting the mode distribution of the planar interface to Eq. (9) of Ref. ⁹, the Kerr-related nonlinear susceptibility of the planar interface is given by

$$\gamma \approx \frac{3\chi_k^{(3)}k_0^2}{4c\varepsilon_0} \frac{1}{(-\varepsilon_m)^{1/2}}, \quad (14)$$

which is independent on the permittivity of the dielectric ε_d . $\chi_k^{(3)}$ is here the Kerr-related nonlinear susceptibility of the bulk dielectric.

IV. DIELECTRIC/HYBRID METAL-FERROMAGNETIC INTERFACE

Next, we consider the dielectric/hybrid metal-ferromagnetic interface as shown in the Fig. 4. In particular such structure has been applied for active magneto-plasmonic micro-interferometry³².

By substituting the mode distribution of a single interface²⁹ into Eq. (7) for the case of the presence of an external magnetic field as in³² we obtain for the plasmon wavenumber shift

$$\Delta k = -\frac{g}{\varepsilon_f} \frac{2h_1(k_0\varepsilon_d)^2}{(\varepsilon_d + \varepsilon_m)(1 - \varepsilon_d^2/\varepsilon_m^2)} \exp(-2k_m h). \quad (15)$$

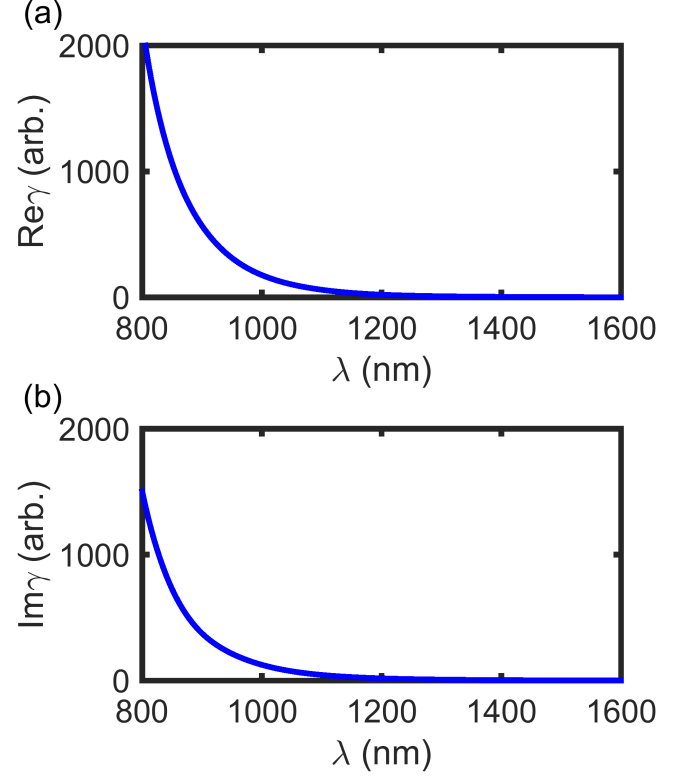


FIG. 5. Wavelength-dependence of the IFE-related nonlinear susceptibility for the interface between the Au-Co-Au hybrid structure and air. The wavelength-dependence of $\chi_g^{(3)}$ is disregarded. (a) and (b) show the real and the imaginary parts of the nonlinear susceptibility, respectively.

Here, ε_f , h and h_1 is the diagonal permittivity, depth and thickness of the ferromagnetic material, respectively, and $k_m = (k^2 - k_0^2\varepsilon_m)^{1/2}$. The Eq. (15) coincides to Eq. (2) of Ref. ³².

Next we consider the case that an incident laser field induces an opto-magnetic field by the IFE. If we substitute the mode distribution to Eq. (10) and assume $\text{Im}\varepsilon_m \ll |\text{Re}\varepsilon_m|$,

$$\gamma \approx \frac{16}{c\varepsilon_0} \chi_g^{(3)} \frac{\text{Re}(\varepsilon_f)}{\varepsilon_f} \frac{\varepsilon_m^4 \varepsilon_d^4}{|\varepsilon_f|^2 (\varepsilon_d^2 - \varepsilon_m^2)^2 (\varepsilon_m + \varepsilon_d)^2} \cdot k_0^3 h_1 \exp(-4k_m h). \quad (16)$$

Fig. 5 shows the wavelength-dependence of the nonlinear coefficient for the interface between the Au-Co-Au hybrid structure and air. Here, we used the experimental data for the permittivity spectra of gold³¹ and cobalt³³ as $\varepsilon_m(\lambda)$ and $\varepsilon_f(\lambda)$, respectively. Fig. 6(a) shows the power-dependence of the nonlinear phase shift ϕ_{NL} for a wavelength of 808 nm and a propagation distance of $L=5000$ nm for the interface between the Au-Co-Au hybrid structure and air. For calculation of the absolute values of the nonlinear phase shift, we assumed $\chi_g^{(3)} = 10^{-17} \text{m}^2 \text{V}^{-2}$. The analytical prediction (the blue

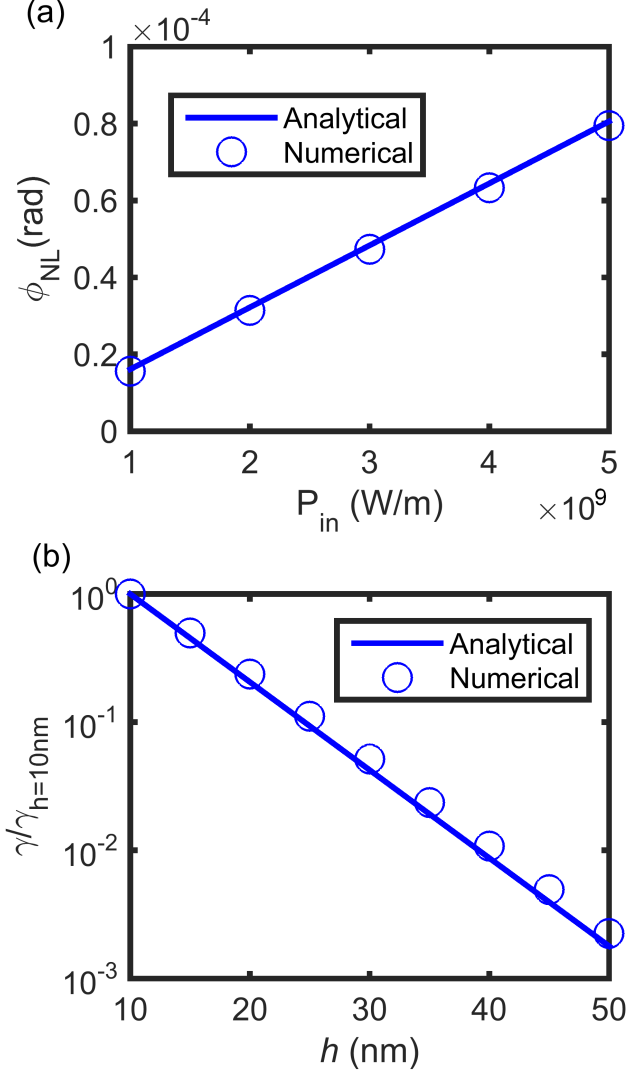


FIG. 6. (a) Power-dependence of the nonlinear phase shift for a wavelength of 808 nm and a propagation distance of $L=5000$ nm for the interface between the Au-Co-Au hybrid structure and air with $\varepsilon_d = 1$, $h = 20$ nm and $h_1 = 4$ nm. (b) Dependence of the nonlinear susceptibility on the position of the cobalt layer. Here, the blue line is calculated by the analytical expression from Eq. (16) and the blue circles are by numerically solving the Maxwell equations in the frequency domain. Here we assumed $\chi_g^{(3)} = 10^{-17} \text{ m}^2 \text{ V}^{-2}$.

line) is in good agreement with the numerical simulation (blue circles). Fig. 6(b) shows the exponential dependence of the nonlinear susceptibility on the position of the cobalt layer in agreement with the numerical simulation, which demonstrates that the nonlinearity originates from the thin cobalt layer.

If we consider $\varepsilon_d \ll |\varepsilon_m|$ in the infrared region,

Eq. (16) is simplified to

$$\gamma \approx \frac{16}{c\varepsilon_0} \chi_g^{(3)} \frac{\text{Re}(\varepsilon_f)}{\varepsilon_f} \frac{\varepsilon_d^4}{|\varepsilon_f|^2 \varepsilon_m^2} k_0^3 h_1 \exp(-4k_m h). \quad (17)$$

As seen the IFE-related nonlinear susceptibility depends on the 4th-power of the permittivity of the dielectric material. For example, by exchanging the air $\varepsilon_d = 1$ with the garnet $\varepsilon_d = 6$ in the hybrid structure Fig. 4, the IFE-related nonlinear susceptibility is enhanced by more than 1000 times. In Ref.³⁴ a possibility has been discussed to increase the magneto-optical effect by increasing ε_d , but the drawback of this approach is the simultaneous reduction of the SPP propagation length. We note, however, the 4th-power-dependence of the IFE-related nonlinear susceptibility on ε_d dominates the reduction of the SPP propagation length. Substituting the mode distribution to Eq. (9) of Ref.⁹, we find for the Kerr-related nonlinear susceptibilities of the structure in Fig. 4

$$\gamma \approx \frac{3\chi_k^{(3)}}{c\varepsilon_0} \frac{\varepsilon_d^3}{\varepsilon_m^3} k_0^3 h_1 \exp(-4k_m h), \quad (18)$$

where $\chi_k^{(3)}$ is the Kerr-related nonlinear susceptibility in the thin layer with the thickness h_1 .

Let us compare the magnitude of the nonlinear phase shift of the hybrid structure of Fig. 4 (including a ferromagnetic metallic layer) with the ferromagnetic dielectric/metal interface in Fig. 1. As seen from the comparison of Fig. 3 with Fig. 6(a) the nonlinear phase shift in the ferromagnetic dielectric/metal interface is by orders of magnitude larger. The reason is that in a ferromagnetic dielectric much more energy is distributed than in a metallic structure.

Note that recently magnetization-induced second harmonic generation has been studied in Ref.^{35,36} arising in magneto-plasmonic systems in the presence of an external magnetic field. The here studied third-order IFE-related nonlinear effect qualitatively differ from this second-order nonlinear effect and do not require any external magnetic field.

Let us discuss the time-response of the IFE-related nonlinearity based on the magnetization dynamics in ferromagnetic thin films. The relaxation process of electrons and spin systems in a ferromagnetic thin films after excitation with a femtosecond pulse is related with a number of processes in the interaction of light with the spin degrees of freedom of electrons and the thermalization of electron in such system. In Ref.²⁶ it was found that a nickel thin film can be demagnetized after excitation by a sub-100fs laser pulse. Several studies confirmed later this result. Note that the underlying mechanism in time-domain magnetization dynamics is still in discussion^{37,38}.

V. DISCUSSIONS AND CONCLUSIONS

Let us estimate the order of magnitudes of parameters for the IFE-related third-order nonlinearity of SPPs in

planar magneto-plasmonic structures. From the expression for the IFE-induced effective magnetic field $\vec{H}_{\text{eff}} = -i\varepsilon_0/\mu_0\beta(\vec{E} \times \vec{E}^*)$ we can predict that the nonlinear susceptibility of a bulk-ferromagnetic material $\chi_g^{(3)}$ is on the order of $\varepsilon_0/\mu_0\beta^2$, where β is the magneto-optical susceptibility. If β is on the order of 10^{-6}m/A^{39} for a ferromagnetic material, $\chi_g^{(3)}$ is on the order of $10^{-17}\text{m}^2\text{V}^{-2}$. This presents a very strong third-order nonlinear susceptibility compared to the Kerr-nonlinearity of typical dielectric materials with $\chi_k^{(3)}$ on the order of $10^{-22}\text{m}^2\text{V}^{-2}$. $\chi_g^{(3)}$ is also larger than the measured $\chi_k^{(3)}$ of gold on the order of $10^{-19}\text{m}^2\text{V}^{-2}$ at the wavelengths of 630 nm⁴⁰ and 796.5 nm⁴¹. If we assume a structure depth on the order of a half wavelength which does not induce noticeable deterioration to the device performance⁴², from Eq. (12) we can estimate a huge nonlinear coefficient γ on the order of $10^6\text{W}^{-1}\text{m}^{-1}$.

In conclusion, in this paper we predicted a new type of ultrafast third-order nonlinearity of SPPs in planar magneto-plasmonic structures based on the induced effective magnetic field by the inverse Faraday effect and its response on the plasmon propagation. We derived a formula for the IFE-related nonlinear susceptibility for two planar magneto-plasmonic structures from the Lorentz reciprocity theorem and analytical expressions for the nonlinear coefficients that describe a strong self-action of the SPPs manifesting in a nonlinear phase shift and a self-induced absorption. Our theoretical prediction of the IFE-related nonlinearity indicates a very large, ultrafast effective third-order susceptibility exceeding those of typical metals like gold. The results presented here could have important implication for the study of magneto-plasmonic systems as well as for applications in nonlinear plasmonics as e.g. to achieve ultrafast plasmonic modulation.

-
- * ryongnam31@yahoo.com or sj.im@ryongnamsan.edu.kp
† jherrman@mbi-berlin.de
- ¹ M. Kauranen and A. V. Zayats, *Nat. Photonics* **6**, 737 (2012).
 - ² K. F. MacDonald, Z. L. Samson, M. I. Stockman, and N. I. Zheludev, *Nat. Photonics* **3**, 55 (2008).
 - ³ M. Mrejen, H. Suchowski, T. Hatakeyama, C. Wu, L. Feng, K. O'Brein, Y. Wang, and X. Zhang, *Nat. Commun.* **6**, 7565 (2015).
 - ⁴ A. Marini and F. Biancalana, *Phys. Rev. Lett.* **110**, 243901 (2013).
 - ⁵ D. V. Skryabin, A. Gorbach, and A. Marini, *J. Opt. Soc. Am. B* **28**, 109 (2011).
 - ⁶ I. De Leon, J. E. Sipe, and R. W. Boyd, *Phys. Rev. A* **89**, 013855 (2014).
 - ⁷ A. Baron, T. B. Hoang, C. Fang, M. H. Mikkelsen, and D. R. Smith, *Nat. Nanotechnol.* **91**, 195412 (2015).
 - ⁸ A. Marini, M. Conforti, G. D. Valle, H. W. Lee, W. C. T. X. Tran, M. A. Schmidt, S. Longhi, P. S. J. Russell, and F. Biancalana, *New J. of Phys.* **15**, 013033 (2013).
 - ⁹ S.-J. Im, K.-S. Ho, Q.-Q. Wang, A. Husakou, and J. Herrmann, *Opt. Express* **24**, 6162 (2016).
 - ¹⁰ A. R. Davoyan, I. V. Shadrivov, and Y. S. Kivshar, *Opt. Express* **16**, 21209 (2008).
 - ¹¹ F. Ye, D. Mihalache, B. Hu, and N. C. Panoiu, *Phys. Rev. Lett.* **104**, 106802 (2010).
 - ¹² A. A. Sukhorukov, A. S. Solntsev, S. S. Kruk, D. N. Neshev, and Y. S. Kivshar, *Opt. Lett.* **39**, 462 (2014).
 - ¹³ A. Kimel, A. Kirilyuk, P. Usachev, R. P. Pisarev, A. M. Balbashov, and T. Rasing, *Nature* **435**, 655 (2005).
 - ¹⁴ C. D. Stanciu, F. Hansteen, A. V. Kimel, A. Kirilyuk, A. Tsukamoto, A. Itoh, and T. Rasing, *Phys. Rev. Lett.* **99**, 047601 (2007).
 - ¹⁵ I. Radu, K. Vahaplar, C. Stamm, T. Kachel, N. Pontius, H. A. Durr, T. A. Ostler, J. Barker, R. F. Evans, R. W. Chantrell, A. Tsukamoto, A. Itoh, A. Kirilyuk, T. Rasing, and A. V. Kimel, *Nature* **472**, 205 (2011).
 - ¹⁶ G. Malinowski, F. D. Longa, J. H. H. Rietjens, P. V. Paluskar, R. Huijink, H. J. M. Swagten, and B. Koopmans, *Nat. Phys.* **4**, 855 (2008).
 - ¹⁷ C. von Korff Schmising, B. Pfau, M. Schneider, C. M. Günther, M. Giovannella, J. Perron, B. Vodungbo, L. Müller, F. Capotondi, E. Pedersoli, N. Mahne, J. Lüning, and S. Eisebitt, *Phys. Rev. Lett.* **112**, 217203 (2014).
 - ¹⁸ F. Büttner, C. Moutafis, M. Schneider, B. Krüger, C. Günther, J. Geilhufe, C. von Korff Schmising, J. Mohanty, B. Pfau, S. Schaffert, A. Biesig, M. Foerster, T. Schulz, C. Vaz, J. Franken, H. Swagten, M. Kläui, and S. Eisebitt, *Nat. Phys.* **11**, 225 (2015).
 - ¹⁹ C. von Korff Schmising, M. Giovannella, D. Weder, S. Schaffert, J. Webb, and S. Eisebitt, *New J. of Phys.* **17**, 033047 (2015).
 - ²⁰ I. I. Smolyaninov, C. C. Davis, V. N. Smolyaninova, D. Schaefer, J. Elliott, and A. V. Zayats, *Phys. Rev. B* **71**, 035425 (2005).
 - ²¹ V. I. Belotelov and A. K. Zvezdin, *Phys. Rev. B* **86**, 155133 (2012).
 - ²² S. Hamidi, M. Razavinia, and M. Tehranchi, *Optics Comm.* **338**, 240 (2015).
 - ²³ V. I. Belotelov, I. A. Akimov, M. Pohl, V. A. Kotov, S. Kasture, A. S. Vengurlekar, A. V. Gopal, D. R. Yakovlev, A. K. Zvezdin, and M. Bayer, *Nat. Nanotechnol.* **6**, 370 (2011).
 - ²⁴ V. V. Temnov, I. Razdolski, T. Pezeril, D. Makarov, D. Seletskiy, A. Melnikov, and K. A. Nelson, *J. Opt.* **18**, 093002 (2016).
 - ²⁵ L. D. Landau, E. M. Lifshits, and L. P. Pitaevskii, *Electrodynamics of continuous media* (Butterworth-Heinemann, Oxford, England, 1995).
 - ²⁶ E. Beaurepaire, J.-C. Merle, A. Daunois, and J.-Y. Bigot, *Phys. Rev. Lett.* **76**, 4250 (1996).
 - ²⁷ L. P. Pitaevskii, *Sov. Phys. JETP* **12**, 1008 (1961).
 - ²⁸ J. P. V. der Ziel, P. S. Pershan, and L. D. Malmstrom, *Phys. Rev. Lett.* **15**, 190 (1965).
 - ²⁹ S. A. Maier, *Plasmonics: Fundamentals and Applications* (Springer, New York, 2007).
 - ³⁰ A. Snyder and J. D. Love, *Optical Waveguide Theory* (Chapman and Hall, London, 1983).
 - ³¹ P. B. Johnson and R. W. Christy, *Phys. Rev. B* **6**, 4370

- (1972).
- ³² V. V. Temnov, G. Armelles, U. Woggon, D. Guzatov, A. Cebollada, A. García-Martín, J. M. García-Martín, T. Thomay, A. Leitenstorfer, and R. Bratschitsch, *Nat. Photonics* **4**, 107 (2010).
 - ³³ P. B. Johnson and R. W. Christy, *Phys. Rev. B* **9**, 5056 (1974).
 - ³⁴ D. Martín-Becerra, V. V. Temnov, T. Thomay, A. Leitenstorfer, R. Bratschitsch, G. Armelles, A. García-Martín, and M. U. González, *Phys. Rev. B* **86**, 035118 (2012).
 - ³⁵ W. Zheng, X. Liu, A. T. Hanbicki, B. T. Jonker, and G. Lüpke, *Opt. Mater. Express* **5**, 2597 (2015).
 - ³⁶ I. Razdolski, D. Makarov, O. G. Schmidt, A. Kirilyuk, T. Rasing, and V. V. Temnov, *ACS Photon.* **3**, 179 (2016).
 - ³⁷ G. P. Zhang, W. Hubner, G. Lefkidis, Y. H. Bai, and T. F. George, *Nat. Phys.* **5**, 499 (2009).
 - ³⁸ K. Carva, M. Battiato, and P. M. Oppeneer, *Nat. Phys.* **7**, 665 (2011).
 - ³⁹ K. Vahaplar, A. M. Kalashnikova, A. V. Kimel, S. Gerlach, D. Hinzke, U. Nowak, R. Chantrell, A. Tsukamoto, A. Itoh, A. Kirilyuk, and T. Rasing, *Phys. Rev. B* **85**, 104402 (2012).
 - ⁴⁰ N. Rotenberg, A. D. Bristow, M. Pfeiffer, M. Betz, and H. M. van Driel, *Phys. Rev. B* **75**, 155426 (2007).
 - ⁴¹ I. De Leon, Z. Shi, A. C. Liapis, and R. W. Boyd, *Opt. Lett.* **39**, 2274 (2014).
 - ⁴² W. Cai, J. White, and M. Brongersma, *Nano Lett.* **9**, 4403 (2009).